AMERICAN UNIVERSITY OF BEIRUT

OPTIMIZING EVAPORATIVE COOLING FOR A REFINERY
FIN FAN COOLER USING COMPUTATIONAL FLUID
DYNAMICS (CFD)

by
JAAFAR IBRAHIM YOUNES

A thesis
submitted in partial fulfillment of the requirements
for the degree of Master of Science
to the Department of Mechanical Engineering
of the Faculty of Engineering and Architecture
at the American University of Beirut

Beirut, Lebanon
August 2021

REPORT OF THE COMPREHENSIVE EXAMINATION
AND THESIS (OR PROJECT) DEFENSE
OF GRADUATE STUDENTS*

To : Registrar

From : Department of Mechanical Engineering

Student's Name : Jaafar Youness ID# 202026023

Major : Energy Studies

I. COMPREHENSIVE EXAMINATION:

The above student sat for the Comprehensive Examination on: April 27, 2021
(Date)
and was evaluated as

Pass
Fail

II. THESIS OR PROJECT DEFENSE:

(a) The Thesis Committee and the Thesis proposal were approved on: April 27, 2021
(Date)

(b) The above student defended his/her thesis/project on: August 23, 2021
(Date)
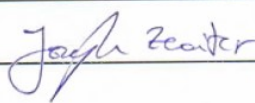and was evaluated as:

Pass
Fail

(c) Following is the exact title of the Thesis/Project:

Optimizing Evaporative Cooling for a Refinery Fin Fan Cooler Using Computational Fluid Dynamics (CFD)

(d) The Examining Committee included the following members:

1. Dr. Kamel Aboughali _____ (Committee Chairperson)

2. Dr. Nesreene Ghaddar _____

3. Dr. Joseph Zeaiter _____

III. REMARKS

Date: Aug. 23, 2021 _____

Signature of Chairperson of Committee

* This form must be completed in full in accordance with University regulations on Graduate Study as they appear in the University Catalogue.
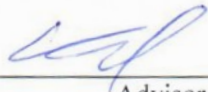
AMERICAN UNIVERSITY OF BEIRUT

OPTIMIZING EVAPORATIVE COOLING FOR A REFINERY
FIN FAN COOLER USING COMPUTATIONAL FLUID
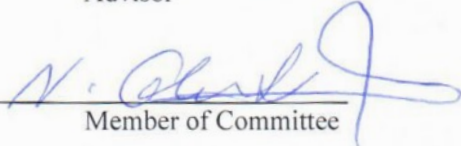DYNAMICS (CFD)

by
JAAFAR IBRAHIM YOUNES

Approved by:

_____

Dr. Kamel Abu Ghali, Professor   Advisor
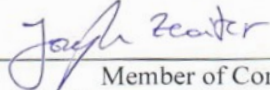Department of Mechanical Engineering

_____

Dr. Nesreene Ghaddar, Professor   Member of Committee
Department of Mechanical Engineering

_____

Dr. Joseph Zeaiter, Associate Professor   Member of Committee
Bahaa and Walid Bassatne Department of Chemical Engineering and Advanced Energy

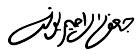Date of thesis defense: August 23, 2021

AMERICAN UNIVERSITY OF BEIRUT

THESIS RELEASE FORM

Student Name: Younes Jaafar Ibrahim

I authorize the American University of Beirut, to: (a) reproduce hard or electronic copies of my thesis; (b) include such copies in the archives and digital repositories of the University; and (c) make freely available such copies to third parties for research or educational purposes:

☒ As of the date of submission

☐ One year from the date of submission of my thesis.

☐ Two years from the date of submission of my thesis.

☐ Three years from the date of submission of my thesis.

_____   August 24, 2021

Signature   Date

ACKNOWLEDGEMENTS

ABSTRACT
OF THE THESIS OF

Jaafar Ibrahim Younes   for   Master of Science
                                                 Major: Energy Studies

Title: Optimizing Evaporative Cooling for a Refinery Fin Fan Cooler Using Computational Fluid Dynamics (CFD)

This study describes three-dimensional computational fluid dynamics CFD simulations of air flow and water droplets through a fin fan cooler assisted with direct evaporative cooling through misting; and proposes an optimized sizing of nozzles resulting in an optimized evaporation process that corresponds to air stream with uniform temperature below or equal to a desired value. The system being studied is a fin fan cooler FFC used in a refinery to cool down a process fluid by forced convection. When the ambient temperature exceeds 34.5 °C, water mist is sprayed into air through 238-uniformly distributed nozzles. Due to high enthalpy of vaporization of water, heat will be extracted from air and hence its temperature is decreased before reaching the tube bundle level. The non-uniform air profile with the current distribution of nozzles is causing non uniform cooling, and hence non uniform temperature profile of air which may result in the lack of performance for the entire process. CFD simulations are run to optimize air temperature just before the tube bundle level by controlling vaporization through proper sizing of nozzles that results in different flow rates of water mist across different nozzles. The location of nozzles was not changed, the size of 14 nozzle in chosen locations was decreased and the size of 11 nozzles at chosen location was increased. The total flow rate of water was preserved. The baseline simulation results showed that temperature reached 34.5 °C in tubes bundle region, but air temperature was not uniform. The optimized sizing plan resulted in uniform air temperature below or equal to 34.5 °C in tubes bundle region.

TABLE OF CONTENTS

ILLUSTRATIONS

Figure

TABLES

NOMENCLATURE

ρ	Density [kg/m^3]
P_{amb}	Ambient Pressure [Pa]
A	Area [m^2]
rH	Relative Humidity [%]
x	Humidity Ratio [g H2O/kg air]
T_{Dew}	Dew Point Temperature [°C]
T_{Sat}	Saturation Temperature [°C]
H	Enthalpy [kJ/kg]
P_v	Vapor Pressure [Pa]
P_{vs}	Saturated Vapor Pressure [Pa]
C_p	Specific Heat [kJ/(kg.K)]
C_v	Specific Volume [m^3/kg]
d	Diameter of Injection Droplets [[μm]
$\bar{d}$	Mean Diameter of Injection Droplets [μm]
Yd	mass fraction of droplets with diameter greater than d [-]
n	Spread Parameter for Rosin-Rammler Function [-]

ABBREVIATIONS

FFC   Fin Fan Cooler

CFD   Computational Fluid Dynamics

DPM   Discrete Phase Model

TBD   Dry Bulb Temperature

WBD   Wet Bulb Temperature

CHAPTER I

INTRODUCTION

Fin fan coolers are large scale heat exchangers that use air as cooling medium to cool down process fluid contained in finned tubes. Fins increase the area of heat exchange, which favors cooling. The system is commonly used in petroleum, petrochemical, and natural gas refineries [1]. Air cooling have the advantages of cost effectiveness, unlimited supply availability of cooling medium, low maintenance, and being non-corrosive. In its basic form, the system is composed of tube bundle that contain the fluid being cooled, air pumping device as axial fan, and a support structure. Headers connect the tubes of the tube bundle and distribute the fluid into them. The tube bundle could be oriented horizontally -which is the most common orientation-, vertically, or within a certain slope. Horizontal orientation of the tube bundle could be achieved in two setups: the forced draft and the induced draft setups. In forced draft setup, the fan is located under the tube bundle and hot air is exhausted from the upper side.

Although forced draft setup is the most used arrangement for its ease of maintenance and lower energy consumption but one of the common problems of this arrangement is accidental warm air recirculation. In the induced draft arrangement, the fan is located above the tube bundle and air is induced through fin tubes. This setup reduces the solar radiation gains by tube, limits air recirculation effects, and allows better airside flow distribution. In certain conditions, where the convection alone is not capable of removing all the needed heat from the process fluid and where environmental

conditions allow, fin fan coolers could be assisted with evaporative cooler that lower the temperature of ambient air.

Evaporative coolers take the advantage of the very high enthalpy of vaporization or the latent heat of vaporization of water which is the amount of energy that must be added to an amount of liquid water to transform it into gas. The high enthalpy of vaporization of water allows the absorption of high thermal energy from surrounding air when the phase change happens (vaporization). This process happens when the highest kinetic energy particles are lost to evaporation, and hence the average kinetic energy of the system being cooled is decreased. The same principle is used by humans and other organisms, they use the evaporation of sweat -which is mostly composed of water- to cool down the body. The enthalpy of vaporization depends on the pressure at which phase transformation happens at.

Evaporative coolers are much lower in energy consumption then compression cycle coolers. In direct evaporative coolers, when unsaturated air meets droplets of water, evaporation takes place and as a result a portion of heat is transferred from ambient air and hence its temperature is lowered. The efficiency of direct evaporative cooling techniques depends on the area of contact between air and water. A widely used method in this field is mist cooling by which very small droplets of water are sprayed into air. Scattered droplets have higher contact area. Other than contact area, efficiency of mist coolers depends on the spraying nozzle type, the droplet diameter, and the climate [2-4].

A. Research Problem

A refinery requires cooling down process fluid from 64.46 to 45.56 °C. Achievement of this objective is to be done within a fin fan cooler by forced convection between air at ambient conditions and the tube bundle that contain the process fluid. For the process fluid to reach the desired temperature, the described system can extract the needed heat only if the ambient temperature of air is below 34.5 °C. The studied fin fan cooler is in induced draft setup where the fans are positioned above the bundle, and they pull air across the fin tubes. This setup reduces the solar radiation gains by tube, limits air recirculation effects, and allows better airside flow distribution as described. Figure 1 shows the general overview of the system.
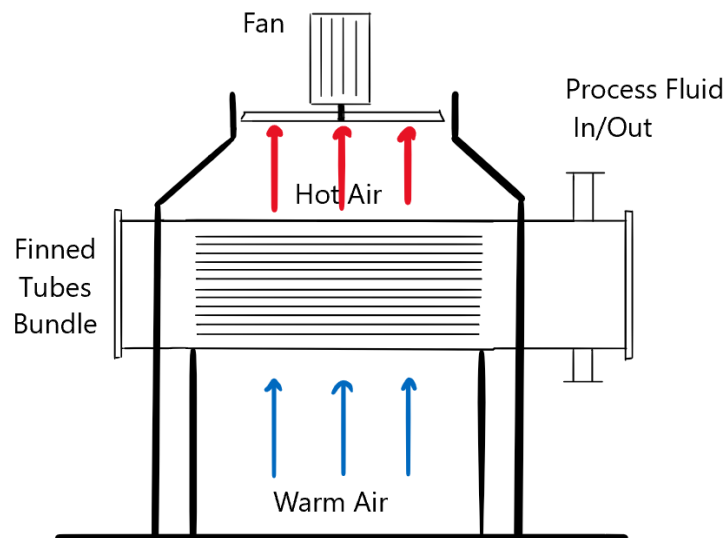
Figure 1 Fin Fan Cooler: Forced Convection Cooling When Ambient Temperature is Below 34.5 °C

If ambient temperature exceeds 34.5 °C, a direct evaporative cooling system is used to lower air's ambient dry bulb temperature to 34.5 °C as shown in Figure 2. The

high enthalpy of vaporization of water allows the absorption of high thermal energy from surrounding air when the phase change happens (vaporization). Misting nozzles are used to spray small droplets of water into air so that evaporation is maximized. The spray system is designed based on the following conditions:

Airflow at Cooler Inlet	200,268 m³/hour
Ambient Dry Bulb Temperature	55 ˚C
Ambient Wet Bulb Temperature	32.2 ˚C
Air Inlet to Cooler Dry Bulb Temperature	34.5 ˚C

Table 1 Water Spray Systems Design Conditions

The current spray system consists of nozzles that are uniformly distributed under the tube bundle as shown in the following figure:
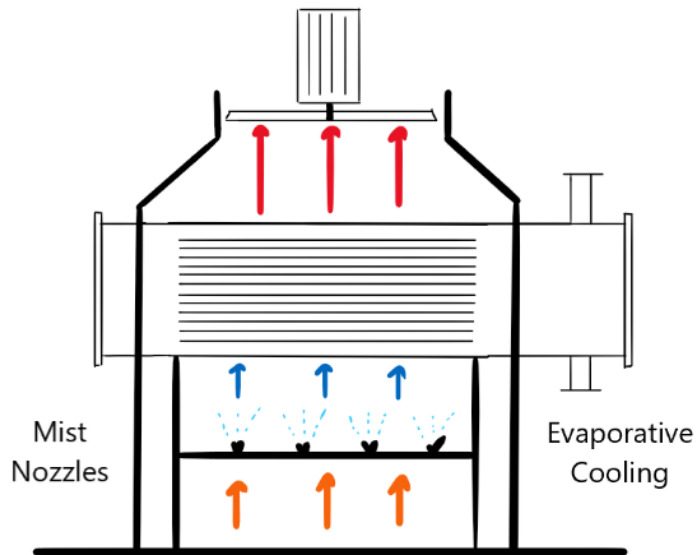
Figure 2 Fin Fan Cooler: Forced Convection Assisted by Direct Evaporative Cooling When Ambient Temperature Exceeds 34.5 °C

B. Objective

The objective is to be met with lowest changes is the design as changes may have financial consequences on the project. Here the importance of CFD simulation appears, where the analysis of CFD results allows achieving the required air flow with least design changes and least financial cost just by the proper sizing of spray nozzles.

The proposed solution to this challenge is optimizing the flow rate of water sprayed through nozzles according to temperature profile of air without evaporative cooling and according to air velocity spectrum in a way that results in a uniform flow within the accepted range of temperature. Therefore, it is recommended to perform a computational fluid dynamics CFD analysis to be able to set flow rate of water through nozzles to achieve this objective. The optimized flow rate of water will be achieved through proper sizing of nozzles in specific locations.

C. Research Design – Methodology

CFD simulation is planned to be done by ANSYS FLUENT, where the simulation will be a multi-phase flow consisting of a continuous phase: air and a discrete phase: water droplets. The common approach used in research for evaporative cooling problems is solving for the continuous phase by Eulerian approach and solving for the dispersed phase by the Lagrangian approach [5-7].

After modeling the system, a baseline simulation is run. The results of the baseline simulation are to be used in designing an optimized design that achieve the desired criterion of uniform temperature profile below 34.5 °C.

The proposed solution for the problem described in research problem section is changing the flow rate of water mist in regions that show (in the baseline simulation) temperature higher than other regions. Increasing the water flow will result in increasing evaporation which will lead to more decrease in air temperature. The humidity ratio or the vapor content of air should be taken into consideration as well because it is possible to have some zones that contain air that is fully saturated with vapor or near saturation, especially that our desired temperature of air is so close to the wet bulb temperature.

 Increasing the flow rate can be achieved in the actual design by changing the nozzle size. Bigger nozzle diameter will result in a higher flow rate for the same setup. The industrial partner provided a table that relates the nozzle size with the flow rate. Hence, flow rate should not be set according to the baseline simulation result only, but it should also depend on the available nozzle sizes. After distributing different nozzles (different in diameter) as described, the simulation is run and the effect of the change is analyzed, if the results do not meet with the desired criterion of uniform temperature

below 34.5 °C, more changes are done according to the result of the optimized case and the same process is repeated.

CHAPTER II

MODELING DEFFIRENT ELEMENTS OF SYSTEM IN ANSYS FLUENT

A. Geometry

The geometry was created as individual parts by SolidWorks. The parts are created based on supplied detailed two-dimension drawings for each part supplied by the industrial partner. After drawing individual parts, all were added into one SolidWorks assembly, then volume extraction was done to extract one body that will be the fluid (air) in the simulation. The part was edited and prepared by ANSYS Space claim before meshing. Every solid element in the real setup was modeled as void to decrease calculations. The boundaries of solids were modeled as a wall as it will affect the velocity of air. The main parts of the fin fan coolers were the tube bundle, the fans, the frame, and other accessories. Parts that have no or have minimal effect on flow were not considered in the simulation as the electric motors and the external frame. The sides of the fin fan cooler were modeled as solid bodies as sheets are to be installed in the actual system.

Figure 3 (a) SolidWorks Assembly File Containing all Individual Parts (b) Sample SolidWorks Part: Section of Tube Bundle

B. Axial Fans Modeling

Two circular surfaces -of 2286 mm diameter each- are drawn in the common surface between the two regions: fluid under and above the fans. Shared geometry is used in SPACECLAIM to indicate that this surface is one surface in the two regions and relevant name selections were given to each element to facilitate the process of meshing and setting fluent boundary conditions later. Internal boundary condition method was used to model the fans. In this method the fan model represents a lumped parameter model that can be used to determine the impact of a fan with known characteristics upon some larger flow field. Using the empirical fan curve provided by fans' supplier Figure 4 and characteristics Appendix 1, the fans are defined by setting the pressure rise across them at steady state conditions.

Inlet Air Density 1,095 kg/m³
355 RPM = 42,49 m/sec
Pressure recovery 0,0000 Inch H2O
Rotor shaft power 9,2 kW
PWL (± 2) 89,1 dB(A)
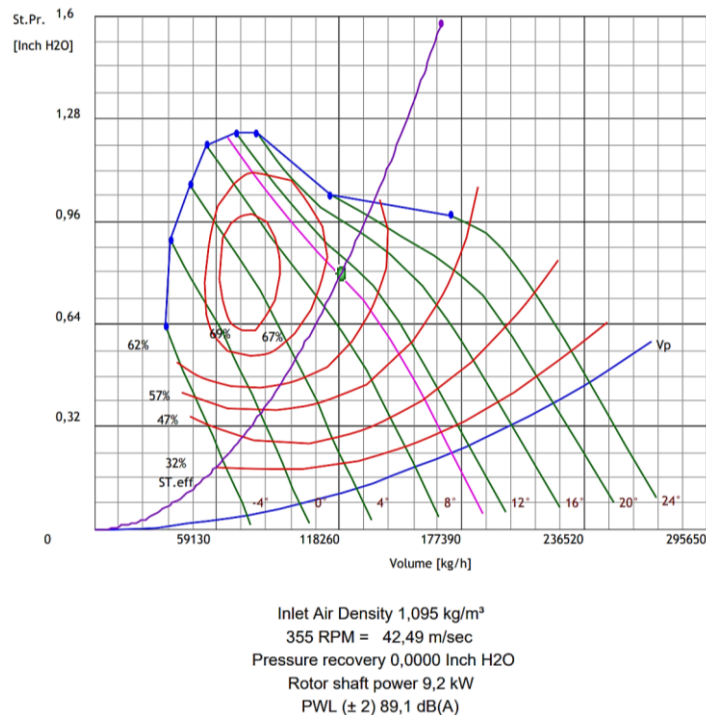
Figure 4 Fan Static Pressure [Inch H2O] vs. Volumetric Flow Rate [Kg/hr.] Curve.

At steady state conditions, the fan will be rotating at 355 rpm with rotor shaft power equals 9.2 kW. At the operation point of the fan, the total efficiency is 75%, fan's static pressure is 0.8 inch of H2O equivalent to 199.34 Pa, the velocity pressure is 0.1145 inch of H2O equivalent to 28.53 Pa and the total pressure rise is 0.9145 inch of H2O equivalent to 227.56 Pa.

Fan model was used instead of sliding mesh as the needed information for defining the fan model as boundary condition are available while some needed information to define the sliding mesh as the accurate geometry of the blades are not supplied. Besides, we are not interested in the description of the detailed flow through the blades but amount of flow through the fan. Hence, the fans are defined by defining the pressure rise across each of them without specifying the radial and tangential components of the swirl velocity, because -as indicated- the detailed flow across the fan is not needed. The pressure jump was set constant as the simulation is for steady state conditions where pressure rise across fans will be constant.

C. Discrete Phase

The discrete phase and the species transport are enabled. Energy equation is turned on. Enabling the discrete phase allows modeling the water droplets as individual elements as indicated and enabling species transport allows transporting water droplets through the continuous phase, air. The mixture of species will be composed of liquid and vapor water, and air gases, mainly nitrogen and oxygen. To specify the humidity of the air entering from the inlet, in the species sub-tab, in boundary conditions tab, the mass fraction of water vapor is calculated from the given wet bulb temperature provided by the industry partner for the site ambient conditions. The industrial partner provided the wet and dry bulb temperatures at the site of installation, then the relative humidity was obtained from psychometric chart to be 21.25% and the humidity ratio -or the fraction by mass of water in air- was found to be 21.349 g-H2O / Kg-air.

D. Meshing

Since the size of the system is relatively large, and it contains very small volumes -as volumes between the tubes-, a good quality mesh as in figure 5b requires a very large number of elements that exceeded 60 million. Increasing the size of element will lower the number of elements but it will result in poor quality mesh in terms of orthogonality and skewness as in figure 5a.

a   b
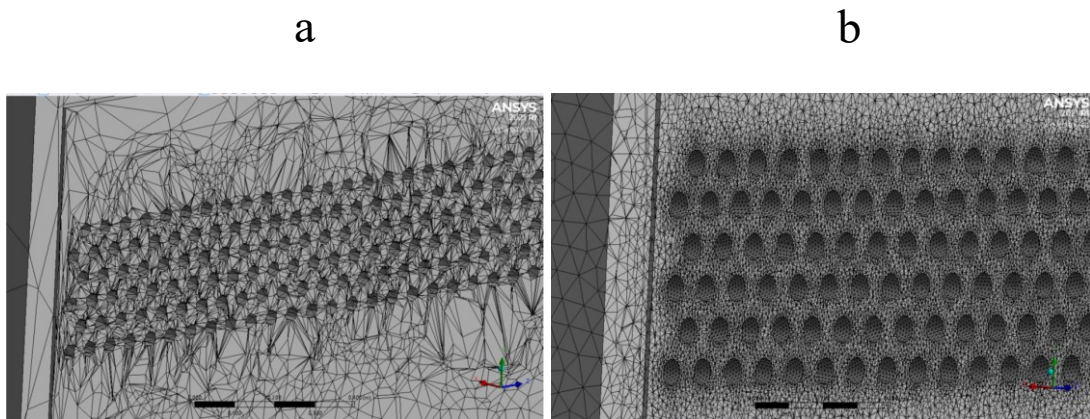
Figure 5 (a) Low Quality Mesh around 2 million Cells: High Skewness (b) High Quality Mesh around 60 million Cells: Low Skewness

Fluent Mosaic Meshing technique was used to create high quality cells in an efficient manner. ANSYS Fluent meshing technology for computational fluid dynamic simulations is a patent pending technique that accelerates the meshing process. Mosaic meshing allows the transition between varying types of mesh elements.
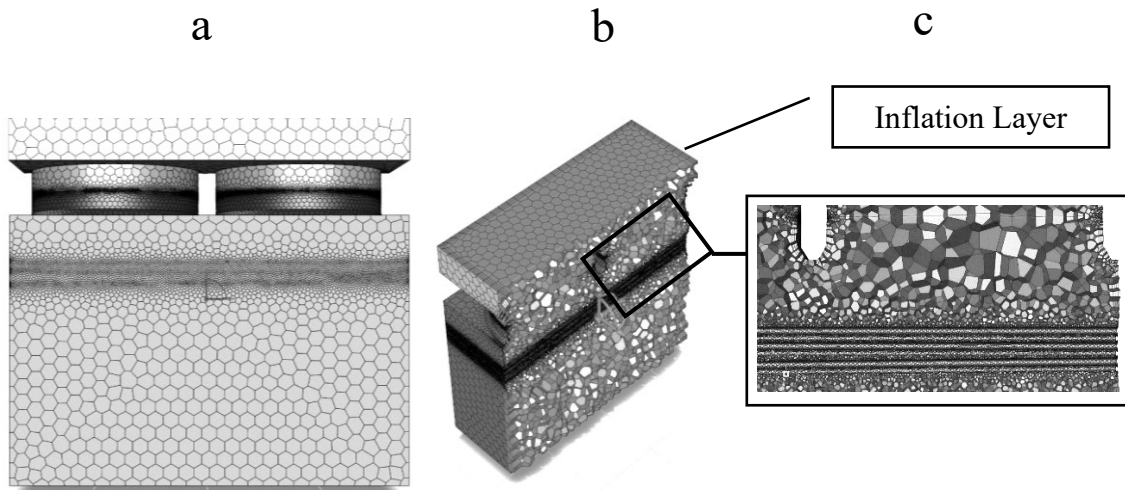
Figure 6 (a) Side View: Mosaic Meshing Technique Used Tetrahedral Cells (b) Section View: Mosaic Meshing Technique (c) Magnified View for Mesh around Tube Bundle

The geometry being meshed consists of only fluid regions with no voids. No control files were used to do the mesh. The minimum size of cells was set to 0.01 m to account for small regions between tubes and the largest size was set to 0.2 meters. The growth rate was set to 1.4. As for the size functions, curvature and proximity methods were used together, by which the curvature and the special location will affect the sizing of the cells. Curvature normal angle was set to 36 so that the circular elements (mainly tubes) will be divided into 10 cells: one cell each 36 °C. Each gap is defined to contain 2 cells. As for proximity, the scope of proximity was set as edges. Hence the sizing will depend on the location from edges. A small inflation layer of 3 layers was used with a transition ratio of 0.272 and a growth rate of 1.2 to provide more detailed flow information near walls where changes are predicted to happen more. The polyhedral shape was chosen as shown in the figures. The following table shows the main indicators for mesh size and quality.

Measure	Value
Skewness (Average)	0.221
Number of Cells	4,099,072

Table 2 Mesh Size and Quality Indicators

E. Injections

Water droplets are modeled as a discrete phase using ANSYS Discrete Phase Model DPM. This technique is used when the aim is to investigate the behavior of the particles from a Lagrangian view and a discrete perspective. The Lagrangian approach deals with each particle separately whereas in Eulerian view, overall diffusion, and convection of a number of particles is calculated [8]. ANSYS Fluent allows 11 different types of injection: single, group, cone, solid-cone, surface, plain-orifice-atomizer, pressure-swirl-atomizer, air-blast-atomizer, flat-fan-atomizer, effervescent-atomizer, and file [9]. As the number of nozzles is large in our study, group or surface injections could be used, but this approach will not allow for optimizing the flow easily, for that reason, all injections are modeled as individual conic injections.

The particles type was set to droplets, the material is set to water liquid, the evaporating species was set H2O, the diameter of water droplets was set using Rosin-Rammler function where the minimum diameter was set to 3.8 microns, the mean diameter $\overline{d}$ was set to 20 microns, and the maximum diameter was set to 48 microns.

The Rosin-Rammler distribution function is a convenient representation of the droplet size distribution based on the assumption that an exponential relationship exists between the droplet diameter and the mass fraction of droplets with diameter greater than d [9].

The complete range of particle sizes is divided into a set of discrete size ranges. The condition of using Rosin-Rammler standard function is having particles that's size ranges between 1 and 200 microns, this condition is valid in our case, hence the standard function was used. The number of diameters for the Rosin-Rammler function was set to 5.

Table 2 represents the mass fraction of droplets of water that have a certain diameter range. Table 3 is created from Table 2. Table 3 represents the mass fraction of droplets with diameter greater than a certain value. This process is used to calculate parameters used to define Rosin-Rammler function for Fluent, namely the mean diameter $\bar{d}$ and the spread parameter n

Diameter d [μm]	Mass Fraction in Range
0 - 3.8	0.05
3.8 - 5	0.05
5 - 10	0.25
10 - 15	0.28
15 - 20	0.1
20 - 25	0.1
25 -30	0.05
30 - 35	0.05
35 - 40	0.05
40 - 48	0.02

Table 3 Injections Droplets Diameter Distribution

Diameter d [μm]	Mass Fraction with Diameter Greater than d, Yd
3.8	0.95
5	0.9
10	0.65
15	0.37
20	0.27
25	0.17
30	0.12
35	0.07
40	0.02
48	0

Table 4 Injections Droplets Cumulative Diameter Distribution
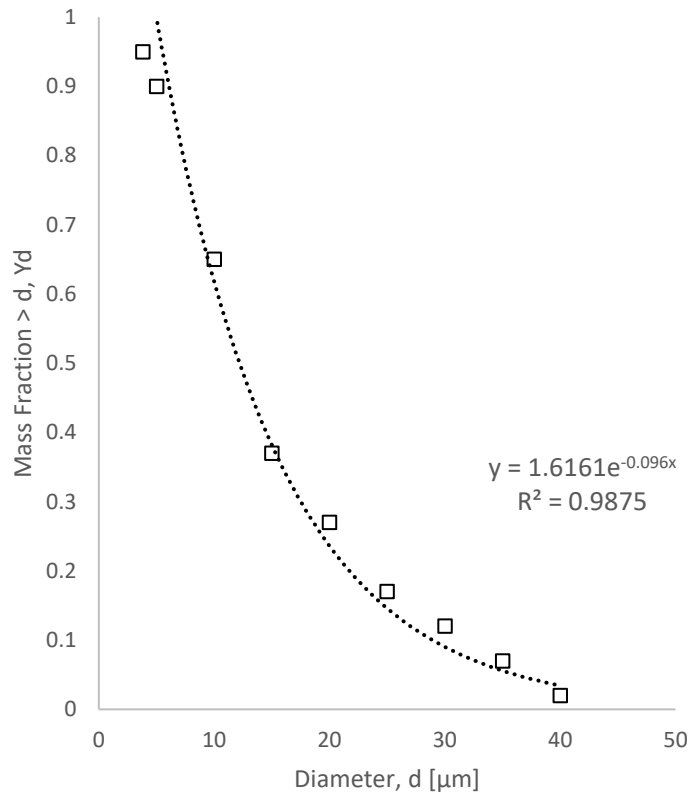
Figure 7 Cumulative Size Distribution of Particles. b. Rosin-Rammler Curve Fit for Particle Size Data

Figure 7 is created from Table 3. The exponential trend line and its equation were found by Excel software.

The mean diameter $\bar{d}$ could be calculated by the diameter which results in Yd = $e^{-1} = 0.368$ [9]. The value obtained for the mean diameter was $\bar{d} = 15.4168\ \mu m$. As for calculating the spread parameter n, it is obtained using the formula:

$$n = \frac{\ln\left(-\ln\left(Yd\right)\right)}{\ln\left(\frac{d}{\bar{d}}\right)}\ [9].$$

In our case, n =7.77345. After obtaining $\bar{d}$ and n, the exponential function is fully defined:

$$Yd = e^{\left(-\frac{d}{\bar{d}}\right)^{n}}\ [9].$$

The spread parameter and the mean diameter in addition to the minimum and maximum diameters are used to define the particle sizing function in ANSYS Fluent. Information about the size of particles were supplied by the nozzle supplier through the industrial partner.
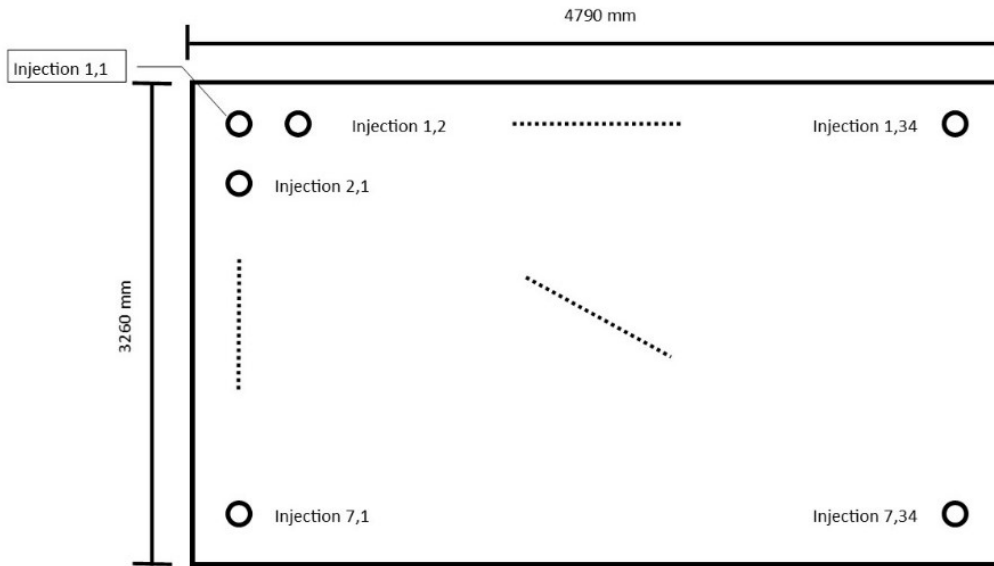
Figure 8 Distribution of Nozzles

Figure 8 shows the distribution of nozzles at XZ plane at Y = 0. The nozzles are distributed in 7 rows and 34 columns resulting in 238 total nozzles. The distance between each two rows is 450 mm and the distance between the rows close to the sides and the sides is 280 mm. The distance between each two columns is 135 mm. The following table shows the distribution of the first two columns of the nozzles.

Column 1			
Nozzle ID	X	Z	Y
0	0.45	0.29	0
1	0.45	0.74	0
2	0.45	1.19	0
3	0.45	1.64	0

4	0.45	2.09	0
5	0.45	2.54	0
6	0.45	2.99	0
Column 2			
7	0.59	0.29	0
8	0.59	0.74	0
9	0.59	1.19	0
10	0.59	1.64	0
11	0.59	2.09	0
12	0.59	2.54	0
13	0.59	2.99	0

Table 5 Distribution of Nozzles in the First Two Columns

Information needed about the spray pattern as the type of the cone, the outer radius, and the angle of the cone were set based on a small experimental setup done for this purpose by the industrial partner. The spray was a solid cone with 45 degrees half angle and 10 cm outer radius.
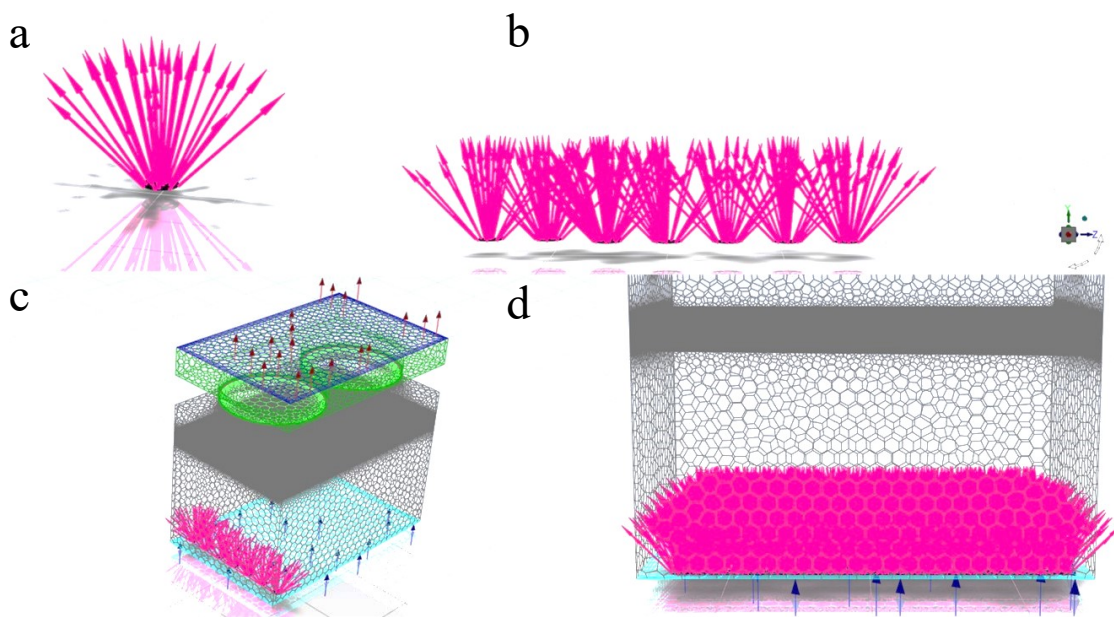
Figure 9 (a) Model of 1 Injection (b) Model of 1 row of injections [7 injections] (c) 1 row of injections shown with the mesh edges outline (d) All injections with lower part of mesh edges outline

F. Boundary Conditions
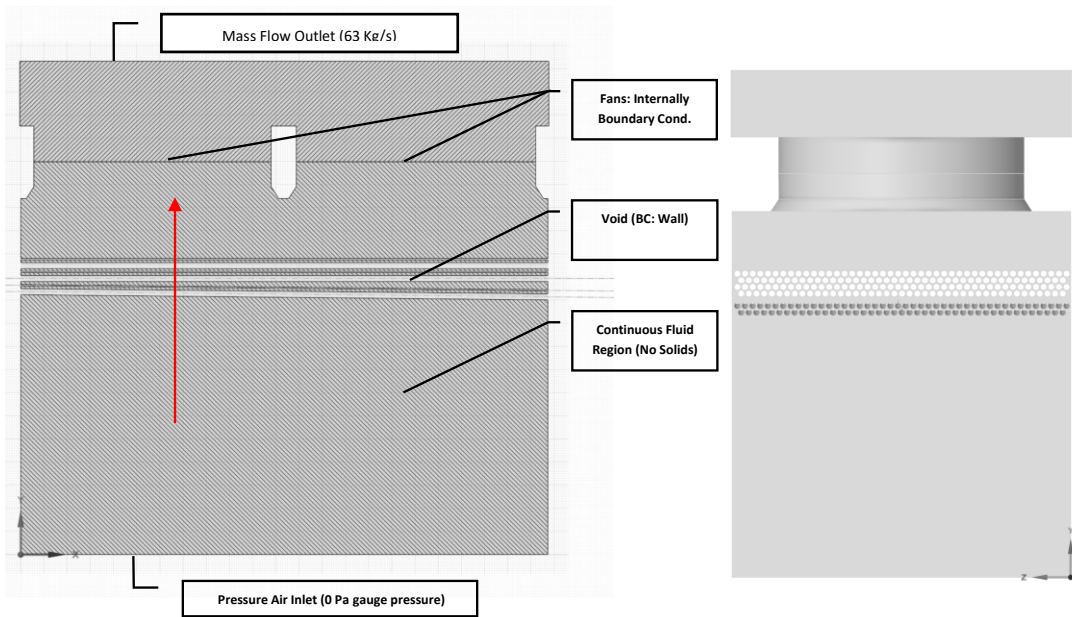
Figure 10 (a) Section View: Fluid Region Representing Continuous Phase (air) Extracted from SolidWorks Assembly File Including Boundary Conditions (b) Side View of The Extracted Fluid
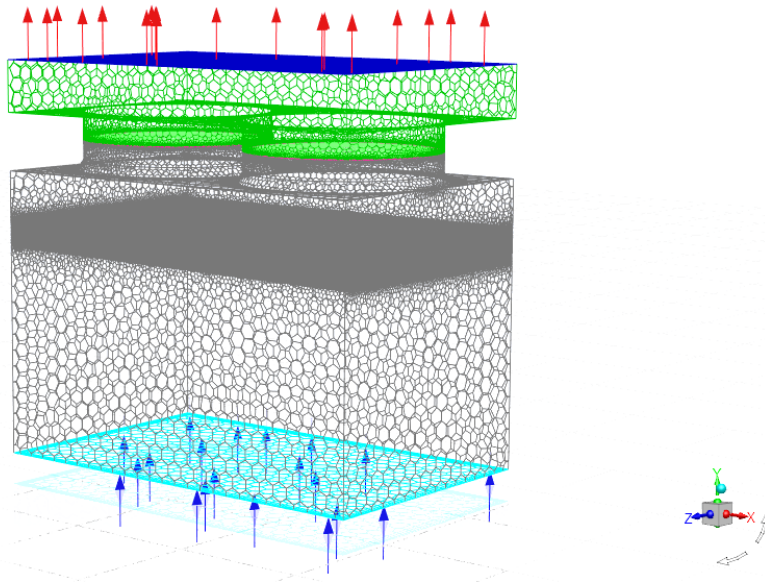
Figure 11 Outline of System's Mesh Including the Boundary Conditions: Dark Blue: Air Mass Flow Outlet, Light Blue: Air Pressure Inlet, Green: Internal Boundary Conditions: Fans; Dark Gray: Walls of Tube Bundle; Light Gray: Walls of Frame

Figure 10 shows the fluid regions in a section view and a side view. The boundary conditions used in this simulation are pressure inlet at the downside of the fin fan cooler, the pressure is set to 0 Pascal gauge pressure equivalent to atmospheric pressure which is the case in the real case. The outlet at the upper side of the cooler was modeled as a mass flow outlet with mass flow rate of 63 Kg/s of air. Since the fan is considered to be infinitely thin, it must be modeled as the interface between cells, rather than a cell zone [9].

As for the discrete phase calculations, the fans were defined as "escape" discrete phase boundary conditions. Water droplets are not predicted to reach fan's levels but if some droplets reach that level, droplets will escape into outside. As for the tubes bundle and the external frame, they all are modeled as walls boundary conditions. The temperature of air entering the cooler is set to 55 °C corresponding to the peak condition faced at the site of installation. The humidity is described in detail in the discrete phase section. The inlet, outlet, and fans boundary conditions are all defined as "escape" discrete phase boundary conditions while walls are defined as "reflect" boundary condition which is the default setting for walls.

G. Simulation Setup

A pressure-based solver is chosen to perform the simulation. As the problem being faced is a steady state problem, and the final objective is to reach a uniform desired profile of temperature at tube bundle level at steady state, the problem is set as a steady state problem. Gravity effect is enabled in this simulation by specifying the direction and magnitude of gravitational acceleration. Gravity is predicted to have affect the discrete phase simulation. As for the turbulence, realizable K-epsilon model (2 equations) is used, and scalable wall functions are used for near wall treatment. K-epsilon model constants are remained in default values. Regarding the solution methods, coupled scheme was used for the velocity-pressure. Hybrid initialization was used. Turbulent kinetic energy terms were relaxed using solutions control with under-relaxation factor of 0.8. Other solution controls were remained default.

The solution was run first for the continuous phase alone. When the solution converged, the discrete phase was enabled.
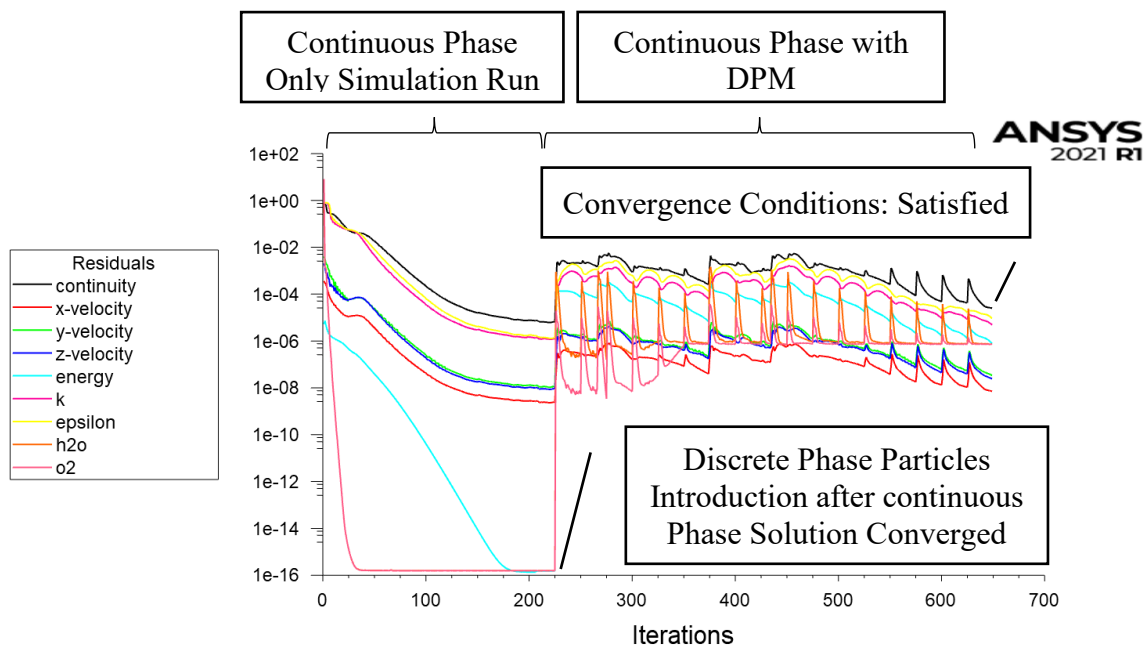
Figure 12 Residuals Plot for Baseline Simulation

30

H. Psychometric Analysis
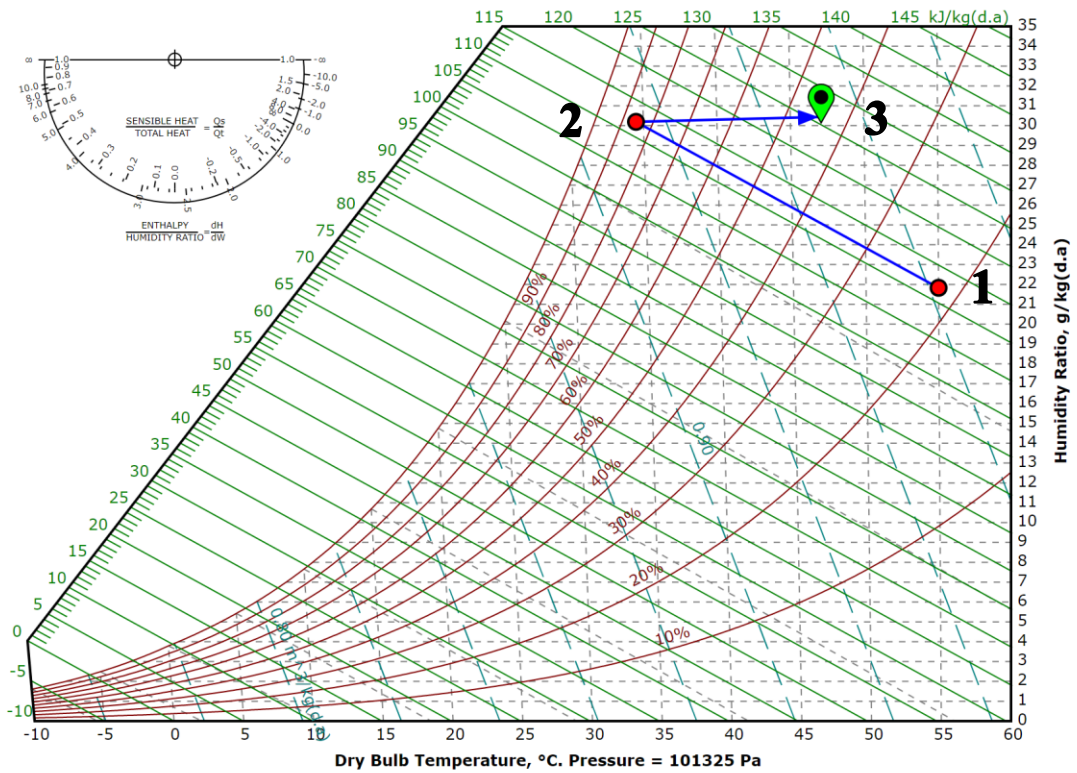
Figure 13 Psychometric chart indicating the air conditions at inlet (point-1) and exit (point-3). Process 1-2: Evaporative Cooling, Process 2-3: Heat Exchange between Air and Tube Bundle

Quantity	1	2	3	Units
Ambient Pressure [P_{amb}]	101325	101325	101325	Pa
Dry Bulb Temperature [TBD]	55	34.5	47.09	°C
Humidity Ratio [x]	21.349	30.141	30.143	g/kg(d.a)
Relative Humidity [rH]	21.252	85.217	43.709	%
Wet Bulb Temperature [WBD]	32.201	32.2	34.491	°C
Dew Point Temperature [T_{Dew}]	25.932	31.65	31.652	°C
Saturation Temperature [T_{Sat}]	31.982	32.178	34.373	°C
Enthalpy [H]	110.836	111.961	125.316	kJ/kg(d.a)
Vapor Pressure [P_v]	3362.53	4683.2	4683.6	Pa
Saturated Vapor Pressure	15759.7	5474.04	10673.2	Pa
Specific Heat [Cp]	1.039	1.04	1.044	kJ/(kg.K)
Specific Volume [Cv]	0.962	0.914	0.951	m^3/kg(d.a)
Density [ρ]	1.062	1.127	1.083	kg/m^3

Table 6: Air Properties at Different Points during Different Processes

As the dry bulb temperature DBT of air is known at exit (assumed equal to the desired value of 34.5 °C) and the wet bulb temperature is known as well (didn't change), the final relative humidity of air leaving the system can be predicted using the psychometric chart before running the simulation and could be used as a validation criterion for the simulation latter. The relative humidity is predicted to be 85.2% at 34.5 °C dry bulb temperature and 32.2 °C wet bulb temperature. This means that by direct evaporative cooling, relative humidity is raised from about 20% to about 85% to decrease the dry bulb temperature from 55 °C to 34.5 °C.

CHAPTER III

BASELINE CASE SIMULATION RESULTS AND DISCUSSION

Figure 14 Results Planes Location: (a) [XZ] plane, y = 2.5 m (just under tubes bundle); (b) [XY] mid plane, z = 1.65 m; (c) [YZ] mid plane, x = 2.61 m; (d) [YZ] plane, x = 1.4 m (center of Fan 1)

Results will be analyzed on 4 different locations shown in Figure 14. The locations are chosen in a way that describe the whole volume. In the following pages contours of air velocity, air humidity ratio, air temperature, water droplets mass flow, and droplet's concentration.

A. Discrete Phase (Water Droplets) Concentration and Mass Flow
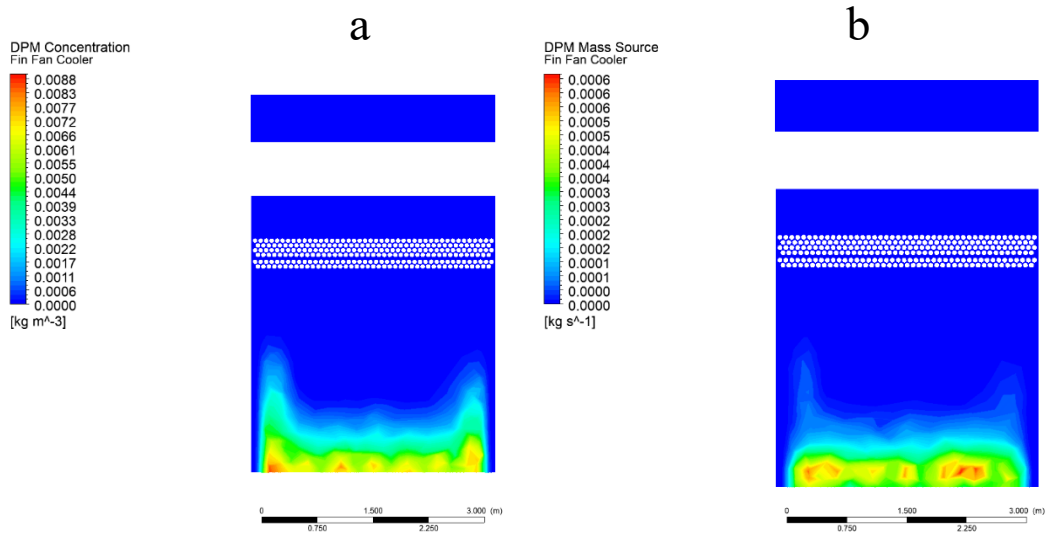
Figure 15 Discrete Phase Model DPM (Water Mist or H2O Droplets) (a) Concentration [Kg/m3] (b) mass flow [kg/s] at [YZ] mid plane, x = 2.61 m
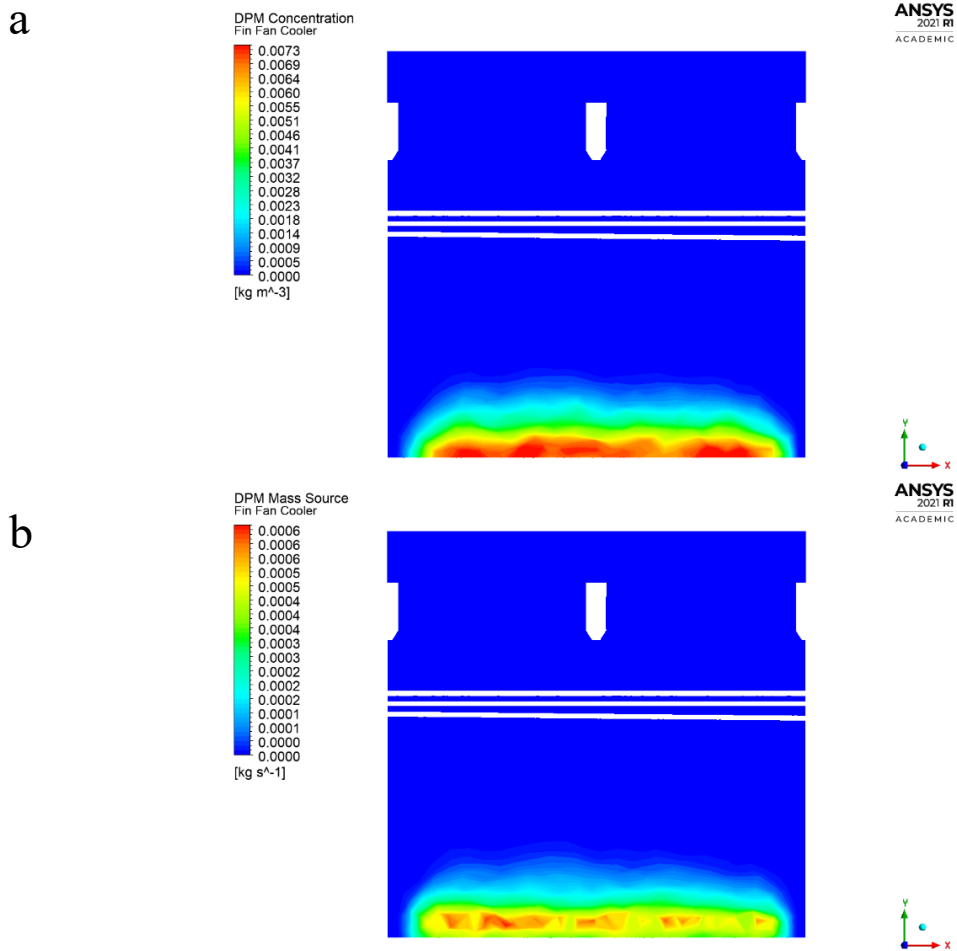
Figure 16 Discrete Phase Model DPM (Water Mist or H2O Droplets) (a) Concentration [Kg/m3] (b) mass flow [kg/s] at [XY] mid plane, z = 1.65 m
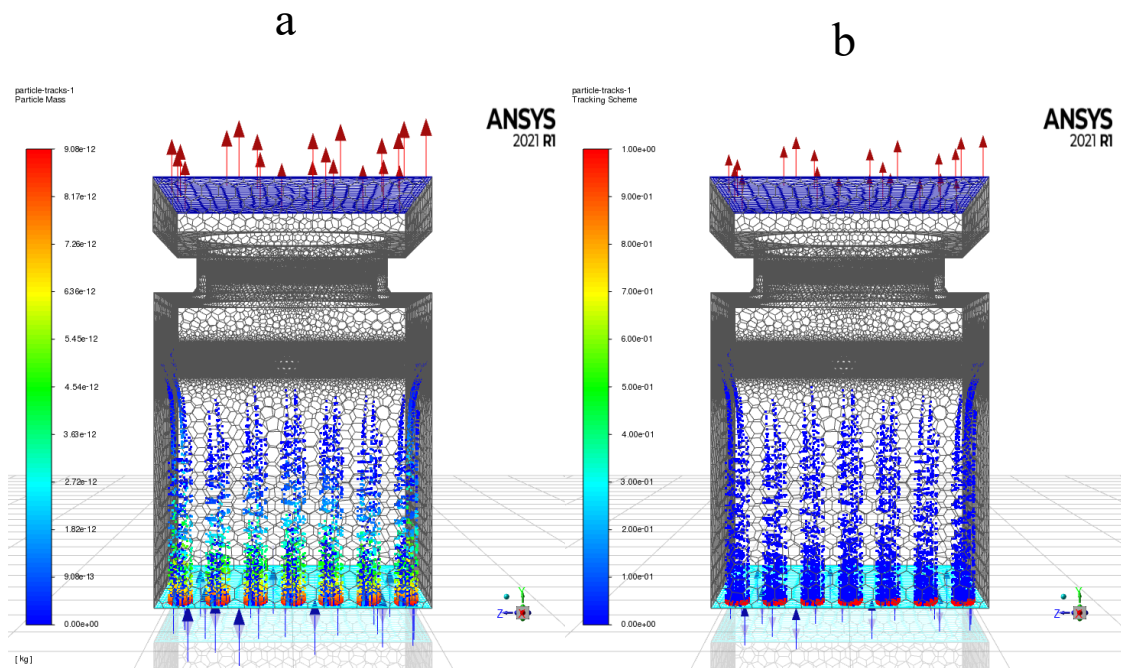
Figure 17 Discrete Phase Tracking: (a) by Particles Mass (b) Tracking Scheme for Droplets Injected from a complete Row of Nozzles at Column 34

Figure 15 (a) and Figure 16 (a) show the DPM concentration in [Kg/m3] at two different locations. Figure 15 (b) and 16 (b) show the mass flow in [Kg/s] at the same locations. Figures 17 (a) and (b) show the tracking scheme by mass and by particle for one complete row of nozzles with the mesh outline. It is noticed that most of the droplet's concentration in the studied location is within the lower part of the fin fan cooler, which is between elevations 0 and 0.5 m (relative to nozzles). The DPM tracking scheme by trajectory and by mass showed that very low portion of mass or of particles (blue color) are reaching high elevations (near the tube bundle) but most of the mass (red and yellow color in Figure 17 (a)) and majority of particles (red color in Figure 17 (b)) are in the lower part. Most of the particles are evaporating at this level

35
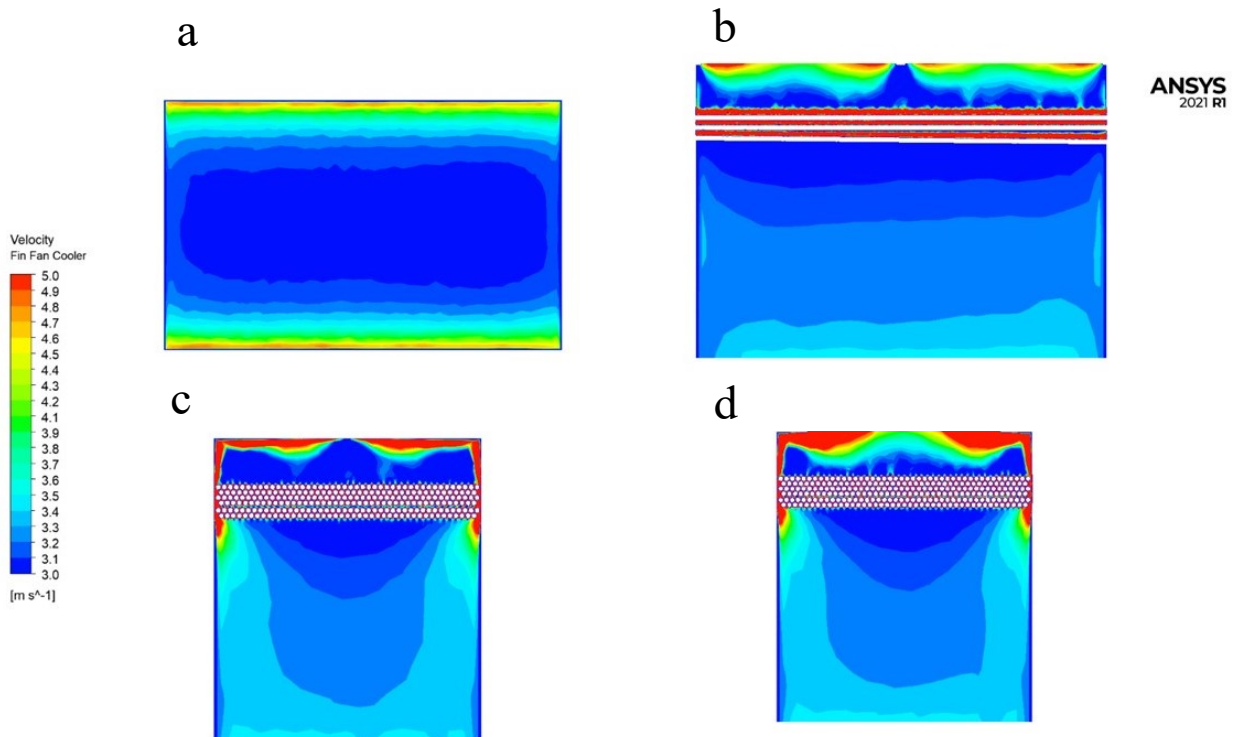
B. Air Velocity

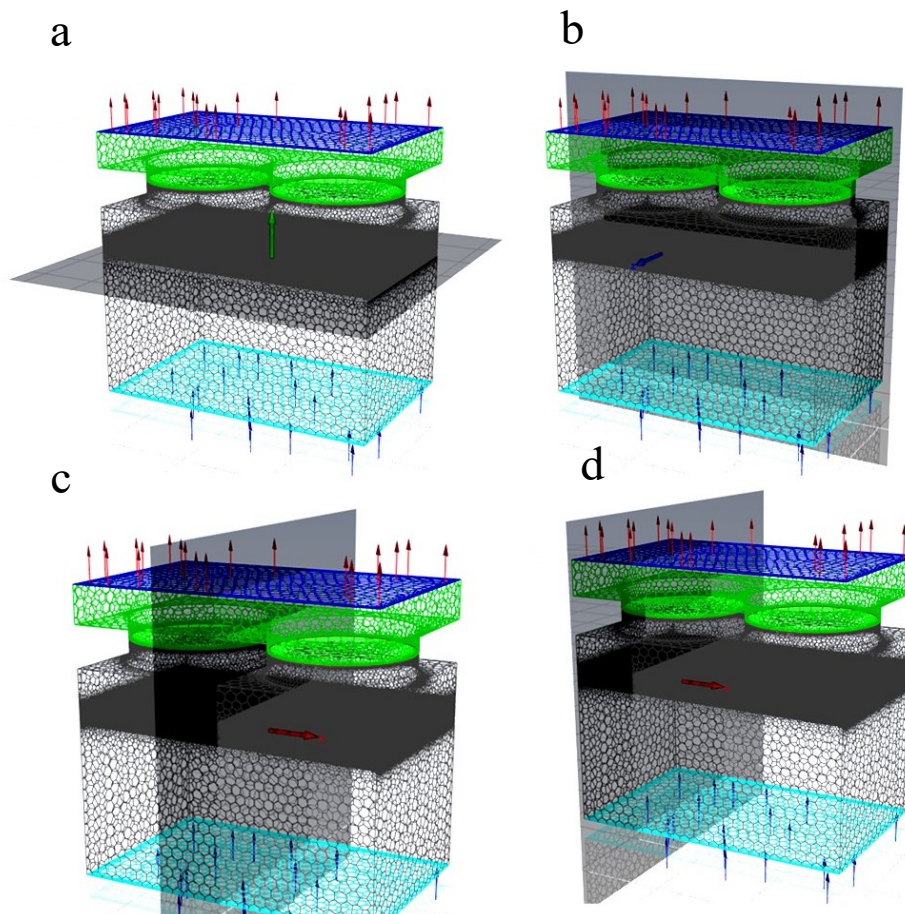
Figure 18 Air Velocity at (a) [XZ] plane, y = 2.5 m (just under tubes bundle); (b) [XY] mid plane, z = 1.65 m; (c) [YZ] mid plane, x = 2.61 m; (d) [YZ] plane, x = 1.4 m (center of Fan 1)

As shown in Figure 18, air in the studied volume has non-uniform velocity profile. In general, air has higher velocity at edges than near center. The figures show air velocity profile with range of 3 - 5 m/s. Some regions encountered much higher velocities as the regions between tubes and near the fan, but the range was made smaller to better describe the velocities in the regions of evaporation. With the non-uniform distribution obtained, evaporation is predicted to be non-uniform, as vaporization rate is dependent on air speed.

C. Air Humidity Ratio
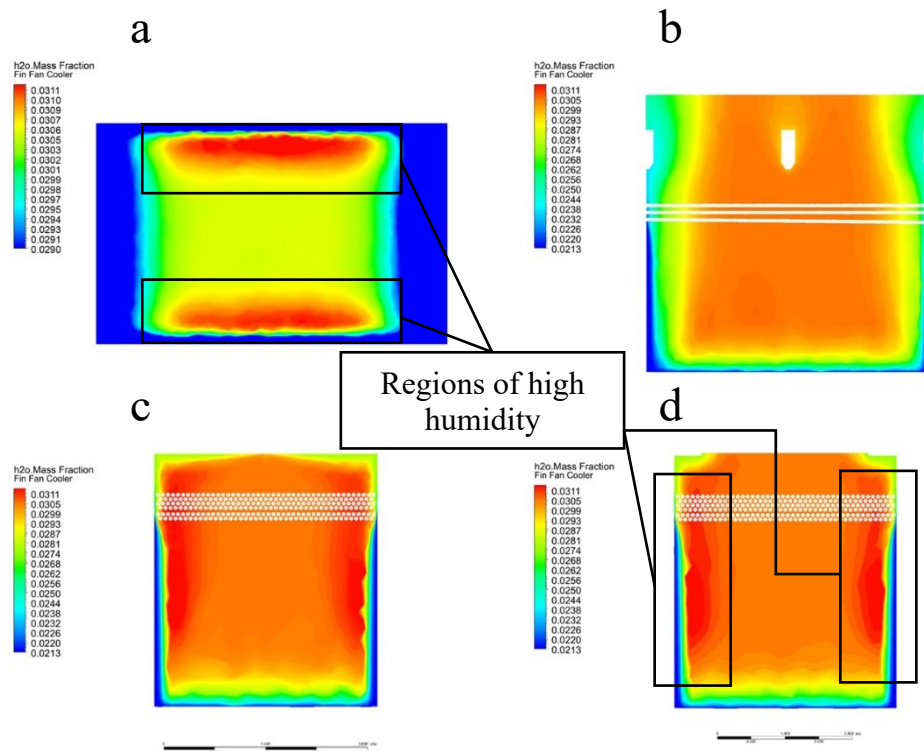
Figure 19 Humidity Ratio [Kg H2O/Kg Air] at [XZ] plane, y = 2.5 m (just under tubes bundle); (b) [XY] mid plane, z = 1.65 m; (c) [YZ] mid plane, x = 2.61 m; (d) [YZ] plane, x = 1.4 m (center of Fan 1)

The results of humidity ratio [Kg H2O/Kg air] show that there are regions that have higher water content than their surroundings. As air at inlet has a uniform humidity ratio of 21.349 g H2O/Kg air, the only conclusion to be drawn is that the regions with high water content (clear in figure 19 (a) and (c) in black rectangles) have gained more water by evaporation than other regions. Evaporation is taking place in these regions more than other regions, meaning that more heat will be extracted by those regions than others, and hence the temperature of air in these regions will be lower than the surrounding. This is the first clear figure that will be used in optimizing the temperature of air flow.

D. Air Temperature
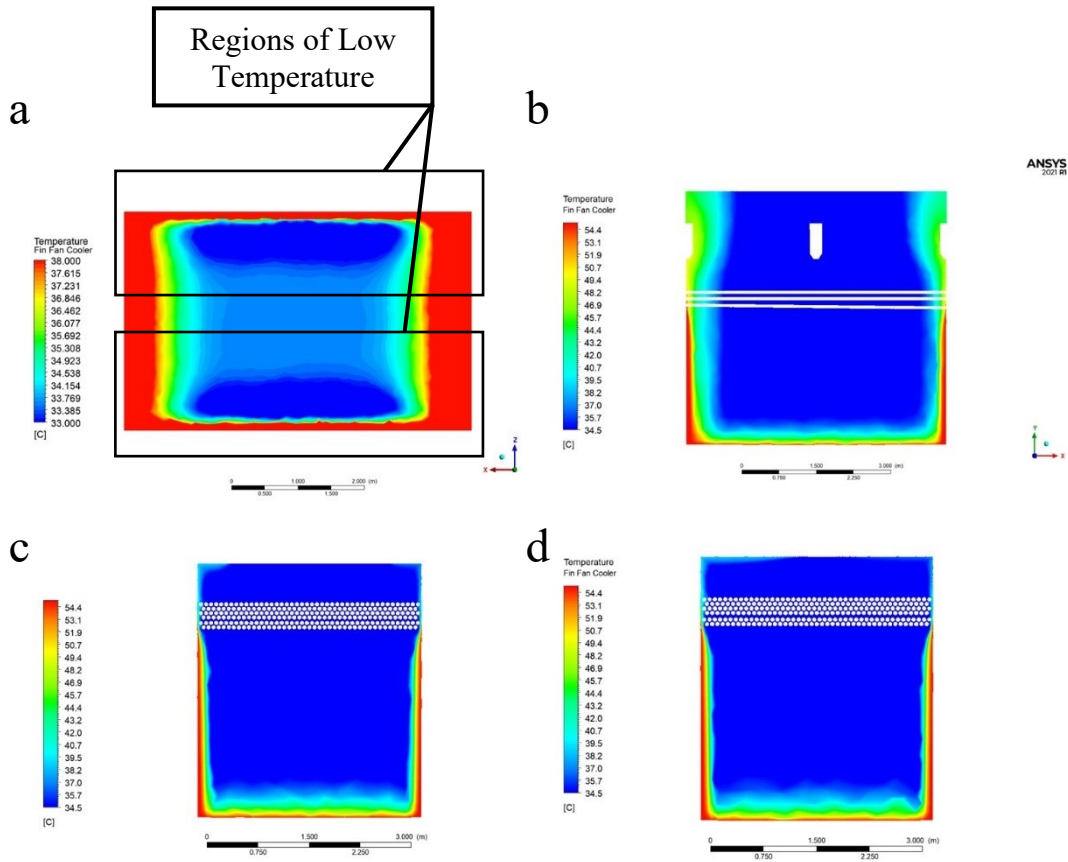
Figure 20 Temperature of Air [°C C] at [XZ] plane, y = 2.5 m (just under tubes bundle); (b) [XY] mid plane, z = 1.65 m; (c) [YZ] mid plane, x = 2.61 m; (d) [YZ] plane, x = 1.4 m (center of Fan 1)

Figure 20 shows air temperature profiles for the 4 studied locations. It is noticed that the objective of having air at a temperature equal or less than 34.5 °C has been achieved without optimization. Although some regions have lost heat more than other regions as described in Figure 19, the temperature in the whole volume was equal or less than 34.5 °C. When this was investigated, the conclusion was that the system is designed with a safety factor.

The amount of sensible heat needed to be extracted from air for its temperature to decrease from 55 °C into 34.5 °C ($\Delta T = 20.5$ °C):

38

$$Q_{sensible} = \dot{m} \, c_p \, \Delta T \qquad\qquad\qquad \text{Eq.1}$$

Where $\dot{m}$ is the mass flow rate of air (63 Kg/s in our case), and c_p is the specific heat of air at 55 °C (1.0077kJ/kg°C in our case).

The energy needed will be around 1301 KW. As this energy is extracted entirely by evaporation, the sensible heat will be equal to the latent heat gained by the flow.

$$Q_{Latent} = \dot{m} \, h_{we} \, dw_{kg} \qquad\qquad\qquad \text{Eq.2}$$

Where h_{we} is the latent heat vaporization of water (2369.8 kJ/kg - in air at atmospheric pressure and 55 °C) and dw_{kg} is the humidity ratio difference (kg water/kg dry air). If the humidity ratio difference is calculated, it will be the amount of water needed to evaporate in order to extract 1301 KW of heat from air:

$$dw_{kg} = \frac{Q_{Latent}}{\dot{m} \, h_{we}} \qquad\qquad\qquad \text{Eq.3}$$

$dw_{kg} = 0.008717$ Kg H2O/Kg air. Multiplying the obtained value by the mass flow rate of air, the amount of water needed will be 0.549 Kg/s or around 33.4 l/min. The industrial partner has used 238 nozzle each with 0.1483 l/min flow, then the total will be 35.3 l/min. The excess amount of water was considered by the industrial partner a safety factor in case an error happened (error may happen due to nozzle flow rate, the supplier provides the flow rate with ±5% error range or from other elements).

The additional amount of water -considered as a safety factor- have led to air with temperature below or equal to 34.5 °C. As the objective of this research is to have

a uniform air temperature as well, Figure 20 (a) shows the temperature of air at XZ plane (parallel to tube bundle).

Temperature range was set between 33 and 38 to better show the variation. It is noticed that the same regions that were more saturated by water in Figure 20 (a) have lower temperature as expected. The regions are located near the long sides of the fin fan cooler. The major cause of this variation is the velocity profile described in Figure 18. The center region, although composes the major space has a higher temperature. Our objective in the next chapter is to have a uniform temperature profile while consuming the same amount of water.

CHAPTER IV

OPTIMIZED CASE SIMULATION RESULTS AND DISCUSSION

To better identify the regions with low temperature / high humidity ratio, 2 plots were created:
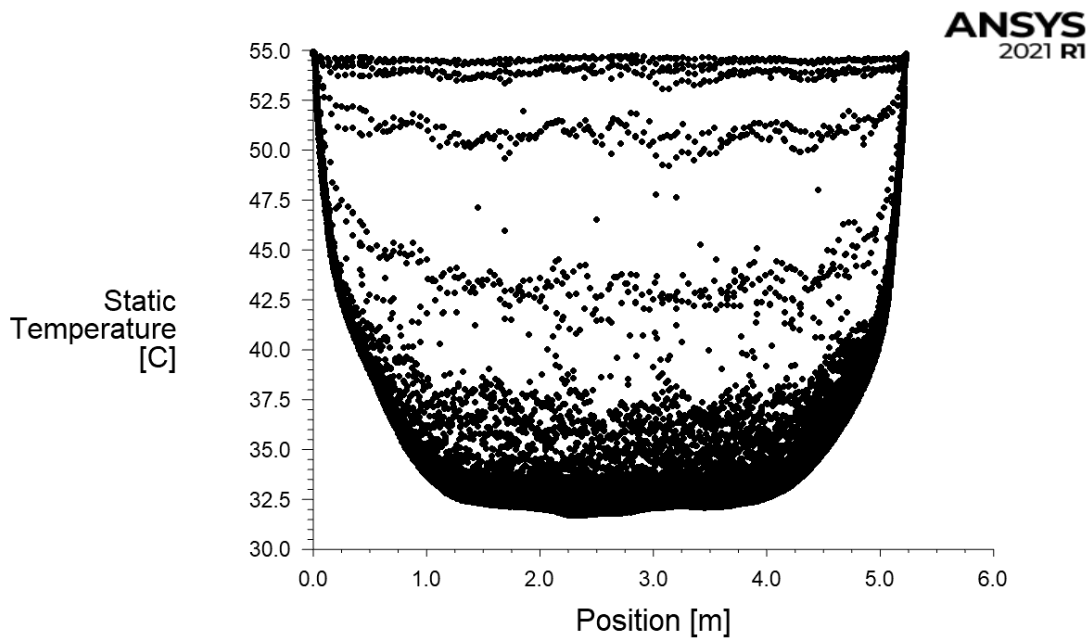
Figure 21 Static Temperature versus x Position (along the long side) in [XZ] plane at 2.5 m elevation (under tube bundle)

Figure 21 is a plot of temperature of different points along the long side of the tube bundle (x-axes in the mesh) at XZ plane at 2.5 meters elevation. The plot shows the temperatures of points located at different x-position. It is noticed that the temperature in this figure is somehow uniform. Most points lay between 32.5 and 35 °C with no high difference between x-position. The conclusion that could be drawn from

this figure is that the position along the long side (x-axis) didn't affect the temperature; a uniform temperature profile exists along x-axis.
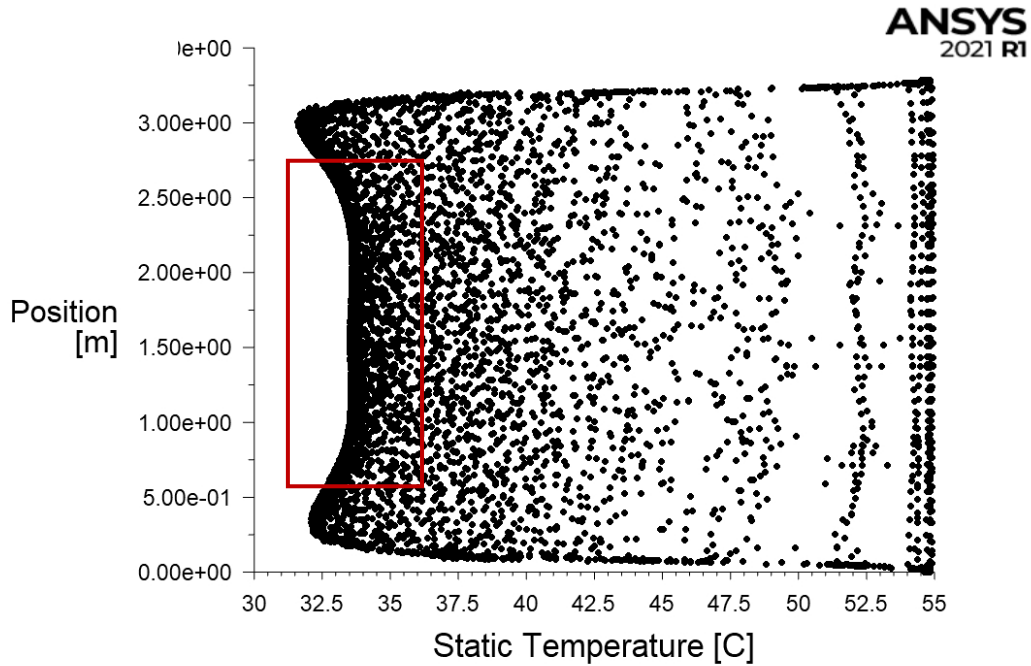
Figure 22 Static Temperature versus z Position (along the short side) in [XZ] plane at 2.5 m elevation (under tube bundle)

Figure 22 shows the temperature variation along the short side in XZ plane at 2.5 m elevation. It is clearly noticed that near the edges, there was a lower temperature than the middle area. The lowest temperature at the middle area was 33 °C while at the two edges, the temperature reached about 32.3 (very close to the wet bulb temperature of air). When air reaches the wet bulb temperature, its relative humidity become 100%, and it will be impossible to hold more water, therefore if more water exists, it will not be evaporated.

To optimize the temperature profile, it is required to decrease evaporation at the two edges and increase it a little in the middle area to have a uniform profile of temperature.

To identify the amount of water needed to be decreased in the edges and redistributed in the middle, the following method was followed:

- The area of low temperatures was estimated using Nitro-pdf software. The area was around 4.95m for the two edges. The ratio of this area to the whole area was 28.5%

- The velocity of air at this area is calculated based on Figure 17 (c) to be 3.4 m/s, density of air at 33°Cis hence the flow rate will be around 1.149Kg/m3, then the mass flow rate of air at the low temperature region will be 20.196 Kg/s which is around 32% of the total mass flow.

- The temperature difference between the low temperature region and the higher temperature region is estimated using the plot in Figure 21. The temperature difference is around 1.5°C. But to estimate the amount of water needed to be decreased in the low temperature region and redistributed, it's needed to estimate the temperature difference between the current low temperature region and the average temperature that will be resulted after redistribution of nozzles in the whole region, it is estimated using the current average to be 1.072°C.

- The excess sensible energy used to extract the additional 1.072°Cis calculated using specific heat of air at 33 °C(1.007 kJ/kg C) to be 21.8KW.Using the heat of vaporization of water at 33 °C(2422.7 KJ/Kg), the amount of water needed to extract this amount of energy from air flow by vaporization is 0.548l/min.

- The industrial partner has provided the following table that shows the flow rate of water mist for different nozzle's size

Nozzle Size [mm]	Flow Rate [Kg/sec]	Flow Rate [l/min]
0.15	0.000766	0.046
0.20	0.001311	0.0787
0.30	0.0018	0.108
0.40	0.002471	0.1483
0.50	0.003366	0.202

Table 7 Flow Rate of Different Nozzle Sizes

The difference in flow between 1 nozzle of 0.4 mm diameter (currently used for all nozzles) and the nozzle with 0.3 mm diameter is 0.0403 l/min

- If the amount of water that is causing the excess cooling and resulting in lower temperature needs to be decreased by changing a number of 0.4 mm nozzles by 0.3 mm nozzles, the number of nozzles that needs to be replaced is calculated by dividing the amount of water needed to be decreased by the difference in flow between nozzles of different size. It is found to be 13.6 nozzles.

- As the fin fan cooler is symmetrical with respect to [XY] plane shown in Figure 13 (b) the number of nozzles to be changed from 0.4 mm to 0.3 mm is 14 nozzles, 7 nozzles from each edge, the nozzles are distributed evenly in the low temperature range to have a uniform temperature profile across edges.

- To preserve the total amount of water initially planned, and to result in a uniform temperature profile for air across the whole area, a certain number of nozzles in the center region are planned to be replaced with bigger nozzles. According to table X the difference in flow between one nozzle of 0.4 mm size and one 0.5 mm nozzle is 0.0537 l/min. If the

same amount of water subtracted from the edges needs to be increased in

the center region, 11 nozzles are needed to be replaced. The nozzles are
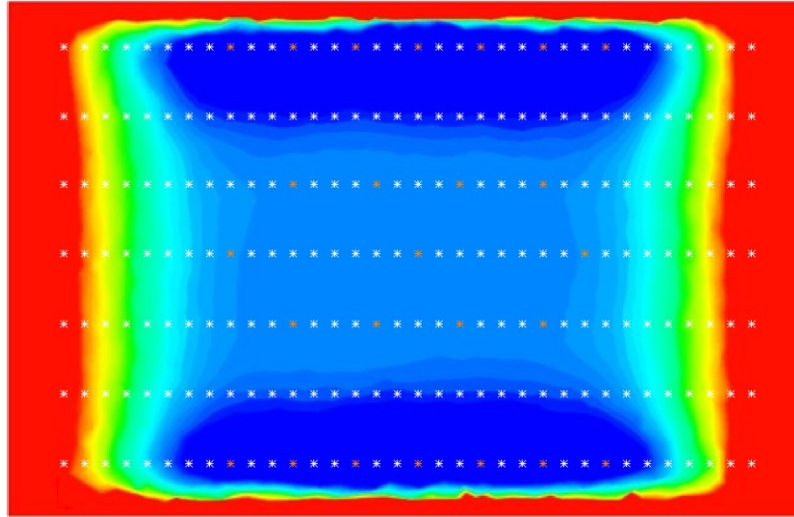
to be distributed evenly in the center region.

Figure 23 Temperature Profile [°C C] in [XZ] plane at 2.5 m elevation with nozzles distribution (Stars); Orange Stars Represent Changed Nozzles

0	7	14	21	28	35	42	49	56	63	70	77	84	91	98	105	112	119	126	132	139	146	153	160	167	174	181	188	195	202	209	216	223	230	
1	8	15	22	29	36	43	50	57	64	71	78	85	92	99	106	113	120	126b	133	140	147	154	161	168	175	182	189	196	203	210	217	224	231	Nozzle Size [mm]
2	9	16	23	30	37	44	51	58	65	72	79	86	93	100	107	114	121	127	134	141	148	155	162	169	176	183	190	197	204	211	218	225	232	0.30
3	10	17	24	31	38	45	52	59	66	73	80	87	94	101	108	115	122	128	135	142	149	156	163	170	177	184	191	198	205	212	219	226	233	0.40
4	11	18	25	32	39	46	53	60	67	74	81	88	95	102	109	116	123	129	136	143	150	157	164	171	178	185	192	199	206	213	220	227	234	0.50
5	12	19	26	33	40	47	54	61	68	75	82	89	96	103	110	117	124	130	137	144	151	158	165	172	179	186	193	200	207	214	221	228	235	
6	13	20	27	34	41	48	55	62	69	76	83	90	97	104	111	118	125	131	138	145	152	159	166	173	180	187	194	201	208	215	222	229	236	

Figure 24 Optimized Nozzles Distribution: White Cells: 0.4 mm Diameter Nozzles (Not Changed), Blue Cells: 0.5 mm Diameter Nozzles (Increased Nozzle Size), Yellow Cells: 0.3 mm Diameter Nozzles (Decreased Nozzles Size)

The new sizes are inserted into the simulation by changing the injections

parameters, mainly the flow rate from the nozzles (based on Figure) and the speed of

water calculated based on the flow rate and nozzle's whole area. The same boundary conditions were used, and the simulation was run again until the solution converged. Results were recorded and the new distribution was successful in causing uniform air temperature distribution. The following figure shows a comparison between the unchanged distribution of nozzle and the optimized distribution:
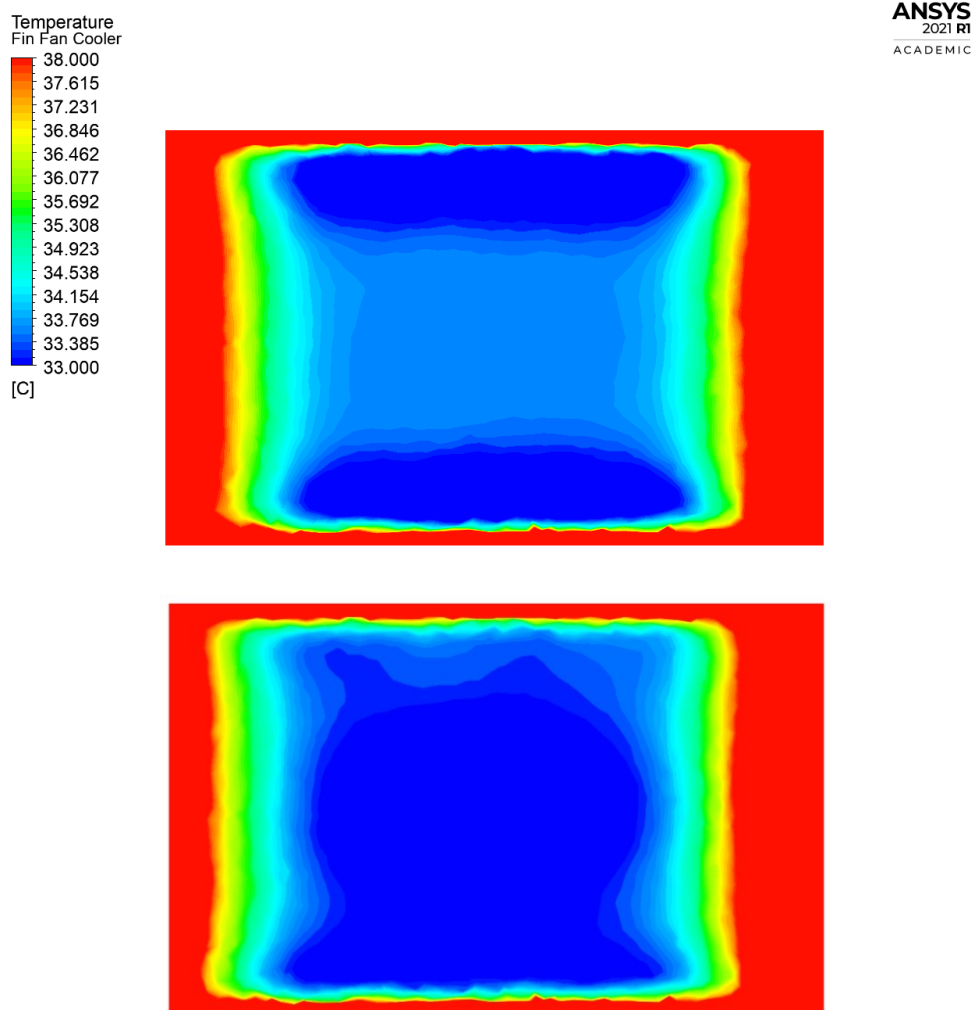
Figure 25 (a) Air Temperature [°C] in XZ Plane at 2.5 m Elevation for (a) Unchanged Nozzle's Distribution and (b) Optimized Nozzle Distribution

Figure 25 shows the difference in air temperature below the tubes for the unchanged and the optimized nozzles distribution. As it is clear that in the unchanged

distribution, two major regions are highly cooled compared to other regions, the

optimized setup has resulted in a uniform distribution across the plane.
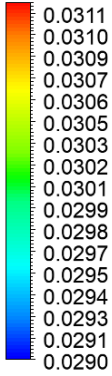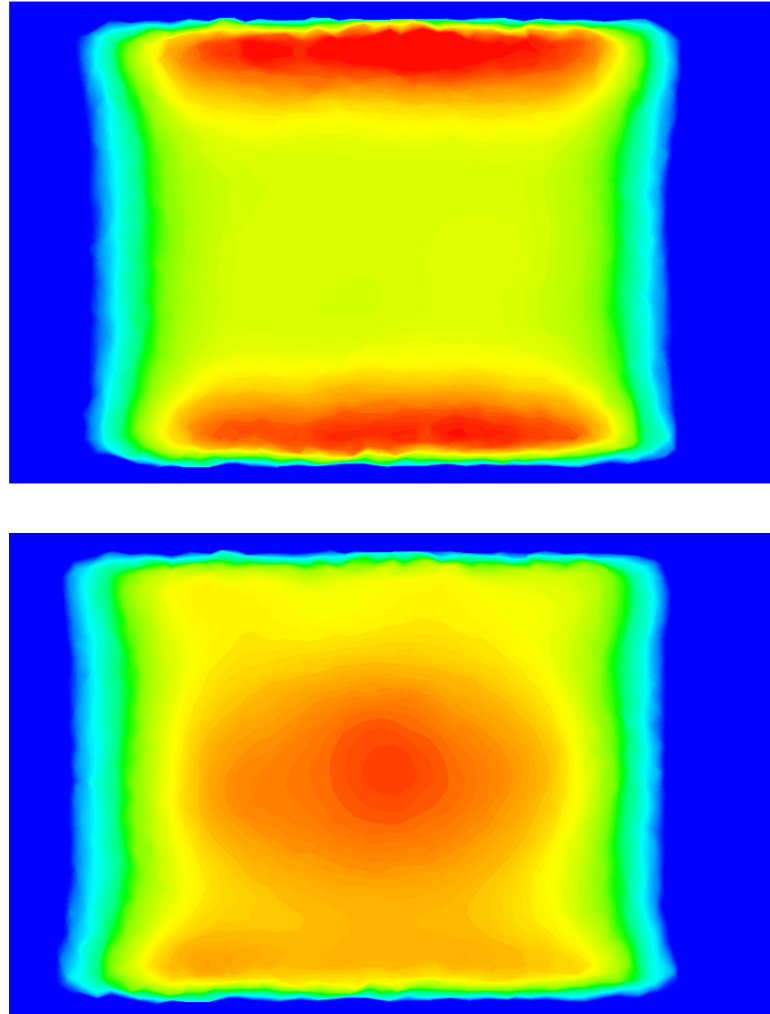
Figure 26 Humidity Ratio [Kg H2O / Kg Air]] in XZ Plane at 2.5 m Elevation for (a)
Unchanged Nozzle's Distribution and (b) Optimized Nozzle Distribution

The same result is shown in Figure 25 where humidity ratio in the unchanged

distribution is concentrated in two regions near the edges, whereas in the optimized

distribution, water saturation was uniformly distributed. Water has reached lower

humidity ratios in the optimized setup compared with the unchanged setup. This is an

advantage because air in the unchanged case is near full saturation which might result in

reaching saturation due to various causes as increase in ambient humidity or changes in

nozzles flow. If air reached full saturation, it will not be able to hold more water in that

region resulting in water sprayed and not evaporated there.
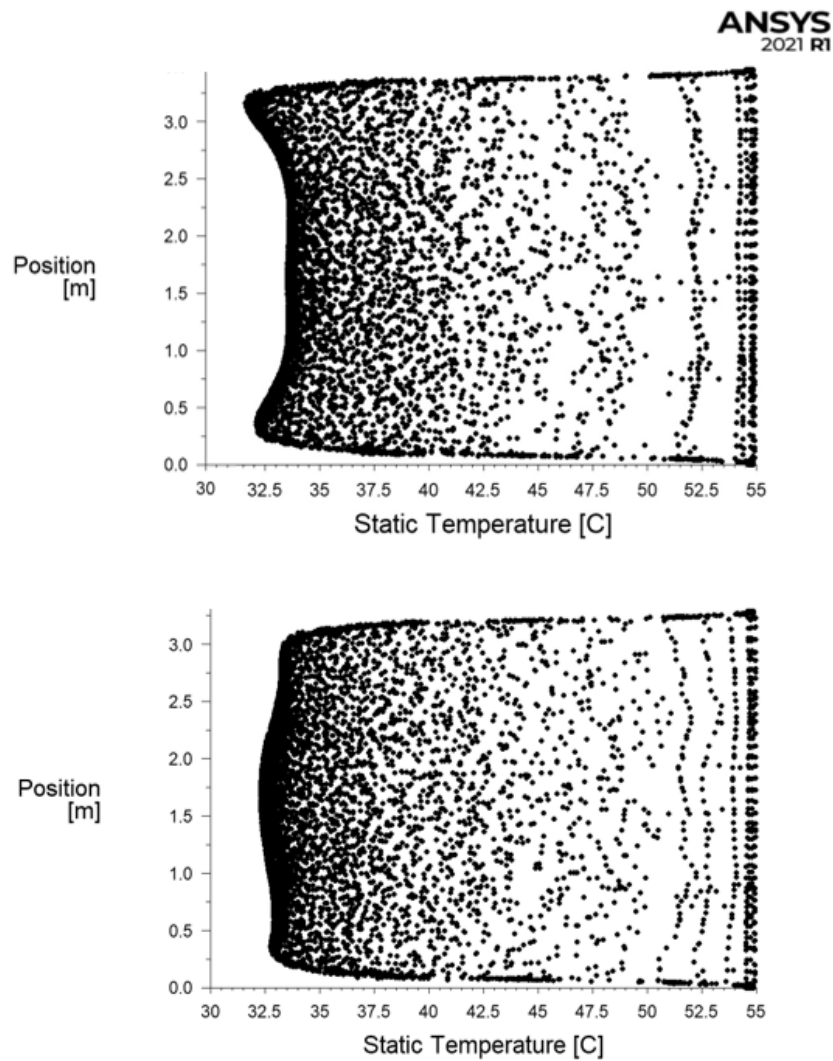
Figure 27 Static Temperature versus z Position (along the short side) in [XZ] plane at
2.5 m elevation (under tube bundle) for (a) Unchanged Nozzles Distribution and (b)
Optimized Nozzles Distribution
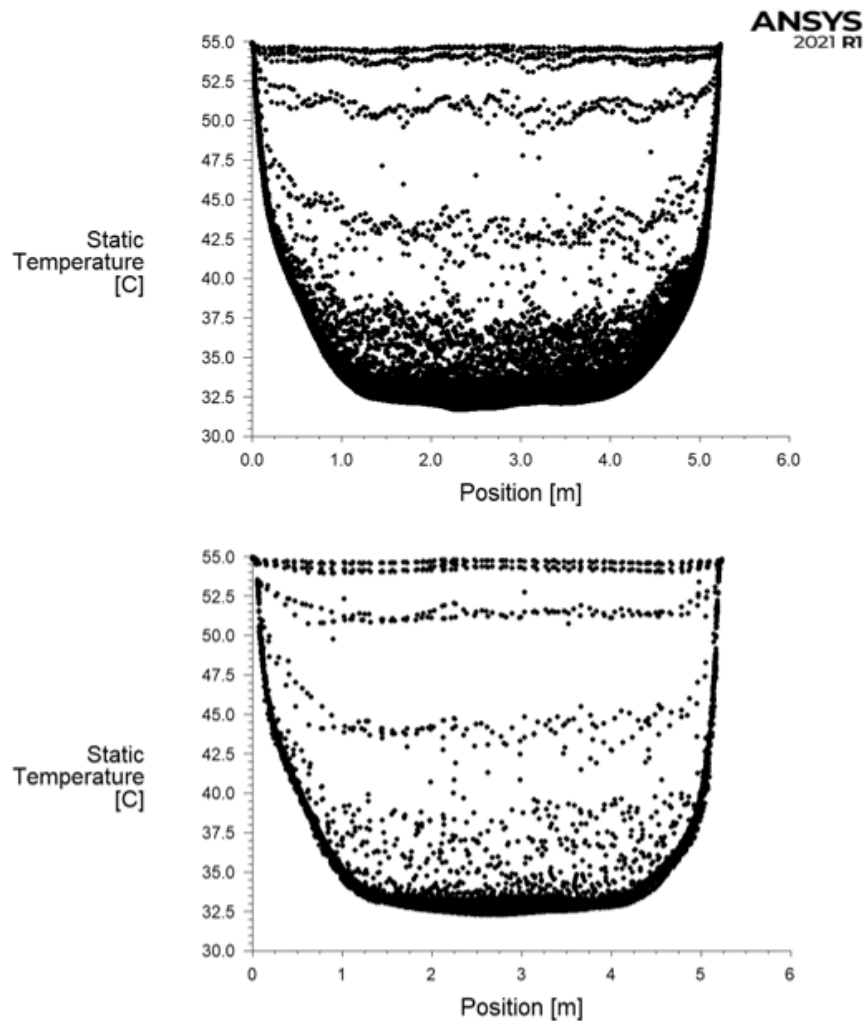
Figure 28 Static Temperature versus x Position (along the long side) in [XZ] plane at 2.5 m elevation (under tube bundle) for (a) Unchanged Nozzles Distribution and (b) Optimized Nozzles Distribution

The same results are shown in Figures 27 and Figure 28. In figure 27 (a) Temperature was very low in two zones: at Z = 0.25 and Z =3 and it was higher in between. In Figure 27 (b) which is the optimized setup, temperature profile was as a vertical line indicating a uniform temperature profile. In addition, the dark black color areas in Figure 27 (a) and Figure 28 (a) are higher than those of Figures 27 (b) and 28

(b) which indicates that the temperature in the optimized setup is more concentrated around 32.5 °C than in the initial setup where temperature is more dispersed. This result is predicted because increasing evaporation -and hence cooling- in two zones will cause decreased cooling in other zones then they will have higher temperature.

To investigate more the uniformity between the two cases, a small statistical comparison was done. Since the values in XZ plane are affected by the walls no slip condition where the temperature is 55 °C and due to the presence of a zone where air temperature is affected by walls region, the temperature range was trimmed and studied between the minimum and 35 °C. The following table summarizes the results:

	Range	Average	Standard Deviation	Variance	Range/ Average
Baseline	3.41	33.41	0.66	0.43	0.1
Optimized	2.7	33.23	0.6	0.37	0.08

Table 8 Statistical Analysis of Air Temperature at XZ Plane at 2.5 m elevation

The range in the optimized case is smaller than that of the baseline case, this shows that the values are within a more squeezed range when optimization was performed. The standard deviation was decreased as well when optimization was applied. Standard deviation of baseline case was 0.66 while in the optimized case it became 0.6. Standard deviation in statistics represents the amount of variation or dispersion of a set of values [11]. Lower standard deviation indicates that the values tend to be closer to the mean of the set, while a higher standard deviation indicates that the values are more spread out over a wider range [11]. The variance was also decreased from 0.43 to 0.37. Variance is a measure of dispersion that reflects how far a set of numbers is spread out from their average [12-13]. Lower standard deviation and

variance reflects clearly the increase in uniformity when optimization plan was applied as the values of temperature became closer to their mean. An additional uniformity measure used is the range over the average. The range over average in the studied set was 0.1 in the baseline case and 0.8 in the optimized case. The conclusion that can be drawn from this index is that the values are closer to the average and their dispersion was decreased when optimized distribution of nozzles was applied.

A final note related to minimum value of air temperature reached is that the value reached in some regions in the baseline case reached the wet bulb temperature WBT. The absolute minimum temperature that could be reached by evaporation is the WBT where the relative humidity of air become 1 and air could not hold more vapor. This regions composes 2% of the total area in the studied XZ plane. In the enhanced design, this temperature was not reached in any region which reflects that the humidity ratio distribution was enhanced and which lowers the probability of reaching full saturation in some regions if certain errors happened (for example if some nozzles provided higher flow rate than rated, etc.).

CHAPTER V

CONCLUSION

The non-uniform evaporation process in an industrial fin fan cooler FFC has resulted in a non-uniform temperature profile in cooling areas. Although the safety factor taken in the design of the FFC has resulted in temperature below 34.5 °C in the region of cooling, but the profiles of air temperature and humidity ratio were not uniform with some regions that became highly saturated with water. If the flow in those regions became fully saturated, evaporation will not take place and water will be uselessly sprayed. This study has provided an optimized setup that results in uniform air temperature and humidity profiles. The optimized setup used the same amount of water used in the baseline case.

Changing the flow rate of sprayed water by changing nozzle's size has resulted in air flow with uniform temperature and humidity ratio. The size of nozzles at different locations was set based on a baseline CFD simulation that modeled the evaporation process in a fin fan cooler FFC through modeling the continuous and the discrete phases. Using CFD, the objective was achieved with least changes to the design and lowest financial consequences.

APPENDIX

Axial Fans Characteristics

CHARACTERISTICS

Required Volume	**119070,00**	kg/h	Required Static Pressure	**0,8000**	Inch H2O
Pressure recovery	**0,0000**	Inch H2O	Fan static pressure	**0,8000**	Inch H2O
Velocity pressure	**0,1145**	Inch H2O	Total pressure	**0,9145**	Inch H2O
Air Temperature	**47,1**	°C	Site Elevation	**250,0**	ft
Inlet Air Humidity (%)			Inlet Air Density	**1,0950**	kg/m³
Fan diameter	**2286**	mm	Fan ring diameter	**2309**	mm
Blade Airfoil	**36N**	ALU	Rotor hub type	**B3**	
Speed	**355,00**	RPM	Blade Tip Speed	**42,49**	m/sec
N. blades	**4**		Blade Operating Freq. +/-5%	**501**	cpm
Static efficiency	**65,6**	%	Total efficiency	**75,0**	%
Blade pitch angle	**10,7**	(°)	Rotor shaft power	**9,2**	kW
Min. Ambient Temperature	**5,0**	°C	Rotor shaft power @ 5,0 °C	**10,6**	kW
			Rotor shaft power @ API point	**12,6**	kW
Pressure Margin (%)	**30**[1] / **54**[2]		Volume Margin (%)	**14**[1]	
Tip Clearance/D	**0,005**		Inlet	**Conical L/D=0.05**	
Diffuser angle (°)			Diffuser:Length/D		
Inlet Obstacle a/A			Inlet Obstacle x/D		
Outlet Obstacle a/A			Outlet Obstacle x/D		
Installation Type	**Induced**		Aerod axial force	**934**	N
Rotor total weight	**79**	kg			
Rotor inertia PD²	**114**	kg x m²			
Max residual unbalance	**18,5**	N			
Blade Failure Load	**7901**	N			
2 Blades Failure Load	**11173**	N			
Xs Static deflection	**70**	mm	Xr Running deflection	**41**	mm

Appendix 1 Axial Fan Characteristics Supplied by Manufacturer

REFERENCES

[1] Rutger Botermans, Peter Smith, CHAPTER 4 - Exchangers, Advanced Piping Design, Gulf Publishing Company, 2008, Pages 83-109, ISBN 9781933762180.

[2] Yamada, H.; Yoon, G.; Okumiya, M.; Okuyama, H. Study of cooling system with water mist sprayers: Fundamental examination of particle size distribution and cooling effects. Build. Simul. 2008, 1, 214–222.

[3] Yoon, G. Study on a cooling system using water mist sprayers; system control considering outdoor environment. In Proceedings of the Korea-Japan Joint Symposium on Human-Environment Systems, Cheju, Korea, 30 November 2008. 35.

[4] Nunes, J.; Zoilo, I.; Jacinto, N.; Nunes, A.; Campos, T.; Pacheco, M.; Fonseca, D. Misting-Cooling Systems for Microclimatic Control in Public Space; PROAP Landscape Architects: Lisbon, Portugal, 2016.

[5] H. Montazeri, B. Blocken, J.L.M. Hensen, Evaporative cooling by water spray systems: CFD simulation, experimental validation and sensitivity analysis, Building and Environment, Volume 83, 2015, Pages 129-141, ISSN 0360-1323

[6] Hamid Saffari, S.M. Hosseinnia, Two-phase Euler-Lagrange CFD simulation of evaporative cooling in a Wind Tower, Energy and Buildings, Volume 41, Issue 9, 2009, Pages 991-1000, ISSN 0378-7788

[7] Rafat Al-Waked, Masud Behnia, CFD simulation of wet cooling towers, Applied Thermal Engineering, Volume 26, Issue 4, 2006, Pages 382-395, ISSN 1359-4311

[8] M.S.Saidi, M.Rismanian, M.Monjezi, M.Zendehbad, S.Fatehiboroujeni, Comparison between Lagrangian and Eulerian approaches in predicting motion of micron-sized particles in laminar flows, Atmospheric Environment, Volume 89, June 2014, Pages 199-206

[9] ANSYS® ANSYS FLUENT 12.1 Documentation, Section 23.3.15 Defining Injection Properties, January 2009.

[10] ANSYS® ANSYS FLUENT 12.1 Documentation, Section 23.3.13 Using the Rosin-Rammler Diameter Distribution Method, January 2009.

[11] Bland, J.M.; Altman, D.G. Statistics notes: measurement error. (1996). BMJ. 312 (7047): 1654. doi:10.1136/bmj.312.7047.1654. PMC 2351401. PMID 8664723.

[12] Math Vault, List of Probability and Statistics Symbols. 2020-04-26. Retrieved 2021-07-25.

[13] Wasserman, Larry (2005). All of Statistics: a concise course in statistical inference. Springer texts in statistics. p. 51. ISBN 9781441923226.